Reentrant phase transition in charged colloidal suspensions: A Monte Carlo study

B. V. R. Tata, Akhilesh K. Arora, and M. C. Valsakumar
Materials Science Division, Indira Gandhi Centre for Atomic Research, Kalpakkam, 603102 Tamil Nadu, India
(Received 17 September 1992)

Monte Carlo simulations of aqueous charged colloidal suspensions interacting via an effective pair potential are carried out with a view to elucidate the mechanism of the reentrant phase transition reported in these systems. The computed pair-correlation functions show that a weakly interacting homogeneous suspension phase separates into dense and rare phases and thereafter reenters into a homogeneous state with crystalline or liquidlike order when the concentration of the ionic impurities is decreased. The cluster-size distribution indeed shows the existence of dense-phase droplets for the intermediate range of impurity-ion concentrations where the phase separation occurs. Some of the recent experimental results are discussed in the light of the present simulation results.

PACS number(s): 82.70.Dd, 64.70.Pf

I. INTRODUCTION

There is considerable current interest in the electrostatically stabilized aqueous colloidal suspensions, in view of the possibility of forming various condensed phases of matter merely by varying the impurity-ion concentration n_i and the particle concentration n_p [1–8]. Recently, a reentrant phase transition has been reported in a dilute aqueous suspension of polystyrene particles [9]. Here, a weakly interacting (gaslike) homogeneous suspension phase separates into concentrated (dense) and dilute (rare) phases as n_i is reduced. This transition is analogous to the well-known vapor-liquid transition in atomic systems. The phase separation occurs only in a certain range of n_i and the suspension is again found to become homogeneous (with crystalline or liquidlike order) as n_i is reduced further. In this paper we report the results of the Monte Carlo (MC) simulations carried out to investigate this reentrant phase transition in a simple one-component model for aqueous dilute charged colloidal suspensions interacting via an effective pair potential.

Until recently it was widely believed that the screened Coulomb repulsion is responsible for the structural ordering in charged aqueous suspensions and that a Derjaguin-Landau-Verwey-Overbeek (DLVO) potential [1] could reasonably well describe the properties of these colloids [10–12]. However, during the last several years more and more experimental evidence is emerging which indicates the existence of an effective attractive interaction at large interparticle separation (several times the particle diameter) which is different from the van der Waals interaction (note that the inclusion of the van der Waals contribution to the interaction potential leads to a primary minimum which occurs at very short distances of the order of a few Å). Some of these are the following: (a) The measured particle concentration in the ordered phase is always significantly higher than the average particle concentration expected for homogeneous dispersion [13–17]. This suggests that the ordered phase does not occupy the entire volume of the suspension. A purely repulsive interaction cannot lead to such a non-space-filling structure. (b) Ordered regions are found to coexist with disordered regions with widely different particle concentrations [18–26]. (c) Stable voids are observed in ordered suspensions [27–29]. (d) Isolated bound pairs are observed in dilute suspension [30] and (e) the phase separation followed by reentrant phase transition upon deionization [9]. These results cannot be explained on the basis of a purely repulsive potential and suggest the existence of attraction, i.e., a secondary minimum in the effective interparticle potential occurring at several times the particle diameter.

Keeping in view the limitations of the DLVO theory, a number of workers have attempted to analyze the charged colloidal suspensions using the integral equation theories [31,32] as well as by employing computer simulations in the canonical ensemble [33,34]. Some of these model calculations predict a weak attraction at very short distances in the effective pair potential for polyvalent counterions or for very large charge densities on macroions. Hence, the attraction resulting from these models cannot explain the observations mentioned earlier [9,13–30] as all these experiments suggest attraction at distances several times the diameter of the particle. Sogami and Ise [35] have presented a formalism for the effective interparticle interaction which uses the adiabatic approximation and the Gibbs ensemble for counterions. It has been shown that a proper statistical mechanical analysis of the counterions lead to an effective attraction between macroions. The resulting pair potential $U_S(r)$ has, in addition to the usual repulsive part, an attractive term which dominates at large interparticle separation. The approximations involved in the formalism and their consequences have been discussed in detail elsewhere [36,37]. Most of the reported results have been understood qualitatively on the basis of this effective pair potential. It may be mentioned that experimental structure factors of liquidlike ordered colloidal suspensions [38], liquid-solid transitions [39], and elastic constants of colloidal crystals [40] have also been explained reasonably well using $U_S(r)$. Therefore, it appears that this potential can be used as a model potential for understanding physi-

cal phenomena in charged colloidal suspensions.

In the present work, consequences of this interaction $U_S(r)$ on the thermodynamic properties of the suspension are investigated using MC simulations. The impurity-ion concentration n_i is varied over a wide range and the state of the suspension is characterized. The system is found to be inhomogeneous, i.e., phase separated into dense and rare phases over a range of n_i and homogeneous outside this range. Clusters of particles constituting the droplets of the dense phase are identified and their size distribution is obtained. The pair-correlation function and osmotic pressure are obtained. The behavior of these quantities is used in identifying the vapor-liquid and reentrant phase transitions. These results are compared with the experimental results reported earlier [9,30].

II. DETAILS OF SIMULATION

MC simulations are done for a canonical ensemble (constant N, V, and T where N, V, and T are, respectively, the number of particles, volume, and temperature). For the required particle concentration n_p, the length L of the MC cell is fixed from the relation $L^3=N/n_p$. Particles of diameter d ($=109$ nm) are assumed to interact via an effective pair potential

$$U_S(r)=2(Ze)^2[\sinh(Kd/2)/Kd]^2 \times(A/r-K)\exp(-Kr)/\epsilon , \quad (1)$$

where $A=2+Kd\coth(Kd/2)$. The inverse Debye screening length K is given by $K^2=4\pi e^2(n_pZ+n_i)/\epsilon k_BT$, where Ze is the charge on the particles, k_B is the Boltzmann constant, ϵ is the dielectric constant of the medium, T is the temperature (298 K), and n_i is the monovalent impurity-ion concentration. This potential has a minimum at $R_m=\{A+[A(A+4)]^{1/2}\}/2K$. Suspensions with n_i ranging between zero and $1000n_pZ$ have been investigated. Table I gives the important parameters of $U_S(r)$, i.e., the position and depth of the potential minimum for the values of n_i considered for simulations.

The simulations are carried out using the well-known Metropolis algorithm [41,42] with periodic boundary conditions. N is chosen to be 432. Simulations are initiated with a body-centered-cubic (bcc) configuration. As the particles are far separated from each other in the initial configuration, an initial step size of $4d$ is chosen to make the system evolve rapidly. Usually, the step size is chosen in such a way that the trial acceptance ratio T_r (the ratio of the number of moves that are accepted to the number of moves that are attempted) is approximately 50% [Ref. 42]. This ensures sampling of the relevant region of configuration space as well as optimization of the equilibration run time. With step size of $4d$, suspensions with n_i in the range $7\le n_i/n_pZ\le 78$ yielded a trial acceptance ratio $T_r\sim 85\%$ initially and it gradually reduced to $\le 25\%$, whereas those with $n_i\le 7n_pZ$ gave $T_r\sim 15\%$. When T_r reached some steady-state value, the step size was lowered to $0.5d$ and the systems were further evolved until equilibrium was reached. With this step size T_r ranged between 40 and 75% for all $n_i\le 78n_pZ$. For suspension with $n_i\ge 100n_pZ$ either of the step sizes gave $T_r\ge 93\%$, exhibiting insensitivity of the weakly interacting system to step size. All the results presented here correspond to final step size of $0.5d$. Values of T_r after reaching equilibrium are shown in Table I. Most of the simulations away from the vapor-liquid transition took 9×10^5 configurations to reach equilibrium, whereas those close to the transition took approximately 5×10^6 configurations to reach equilibrium. Constancy of the average total interaction energy U_T $[=\frac{1}{2}\sum_{i\neq j}^{N}U_S(r_{ij})]$ is taken to be the criterion for reaching equilibrium.

After reaching equilibrium, $g(r)$ is calculated (for $r\le L/2$) using the standard methods [43]. The interval Δr is taken to be $0.1d$ and averaging was performed over configurations generated from 550 Monte Carlo steps (MCS's) (one MCS consists of a set of N configurations, where on the average each particle gets a change to move). Osmotic pressure P^*, expressed in units of n_pk_BT ($P^*=P/n_pk_BT$), is calculated using the virial equation [2,42]. A cluster of dense phase is defined in a conventional manner [44]. Here, constraining volumes of radius R_c are marked around each macroion. A given macroion

TABLE I. Inverse Debye screening length (K), position of potential minimum (R_m), the depth of the potential well (W), first peak position R_p of $g(r)$, and equilibrium trial acceptance ration (T_r) for different impurity-ion concentrations (n_i).

n_i/n_pZ	Kd	R_m/d	$W=-U(R_m)/k_BT$	R_p/d	T_r (%)
0	0.27	18.12	0.30	9.1	50
1.5	0.42	11.50	0.47	8.7	68
2.0	0.46	10.46	0.51	8.5	72
2.6	0.51	9.57	0.56	8.3	75
3.0	0.53	9.13	0.58	8.1	76
5.0	0.65	7.49	0.71	7.1	82
7.0	0.76	6.52	0.80	6.1	80
10.0	0.89	5.60	0.92	5.2	75
30.0	1.49	3.49	1.32	3.3	55
78.0	2.38	2.40	1.51	2.2	40
100.0	2.69	2.21	1.49	2.2	92
150.0	3.28	1.95	1.39	1.95	93
400.0	5.35	1.55	0.86	1.55	96
1000.0	8.45	1.35	0.42	1.33	99

belongs to a cluster if the neighborhood of that macroion has nonzero overlap with the neighborhood of at least another one belonging to that cluster. R_c is taken to be the distance at which the minimum of $g(r)$, after the first peak, occurs. This is reasonable as it takes care of the spread in the nearest-neighbor distance and hence all the first neighbors get included. Having identified all the clusters, their size distribution $\rho(n)$ and the total fraction of particles participating in the clustering F_c (the total number of particles participating in the clusters/N) are obtained.

III. RESULTS AND DISCUSSION

Figure 1 shows the pair potential $U_S(r)$ for different n_i values for suspensions with $n_p = 1.33 \times 10^{12}$ cm^{-3}. The charge on the macroion Ze is taken to be $500e$, which is the same as the value reported [6]. The vertical line in Fig. 1 denotes the average interparticle spacing $a_s = n_p^{-1/3}$. Note from Table I that the depth W and the position R_m of the well depend strongly on n_i. It is clear from Fig. 1 that the dispersion will be homogeneous when $R_m > a_s$. The structural ordering in this homogeneous state depends upon the strength of the potential at $r = a_s$. However, when $R_m < a_s$ the system can, in principle, phase separate into dense- (particle concentration higher than n_p) and rare- (particle concentration lower than n_p) phase regions, provided W is sufficiently large.

Figures 2–4 show the pair-correlation functions for various impurity-ion concentrations ranging between zero and $1000 n_p Z$. Note from Fig. 2 that for $1000 \geq n_i/n_p Z \geq 100$ there is a single peak in $g(r)$ at a position R_p which is close to that of R_m. Also, the pair-correlation function saturates to one immediately after the first peak, suggesting that there are no short-range structural correlations. As seen in Fig. 3, the $g(r)$'s obtained for suspensions with impurity-ion concentration in the range $78 \geq n_i/n_p Z \geq 7$ are markedly different from those at high n_i. These have several peaks in $g(r)$ which suggest structural correlation up to several neighbor distances. However, the first peak position still corresponds to the minimum of the potential well. Further, the heights of the first peak are very large, e.g., 80 in the case of suspension with $78 n_p Z$, and $g(r)$ gradually decays to one as r increases. This type of behavior is expected only when dispersion is inhomogeneous. Suspensions with

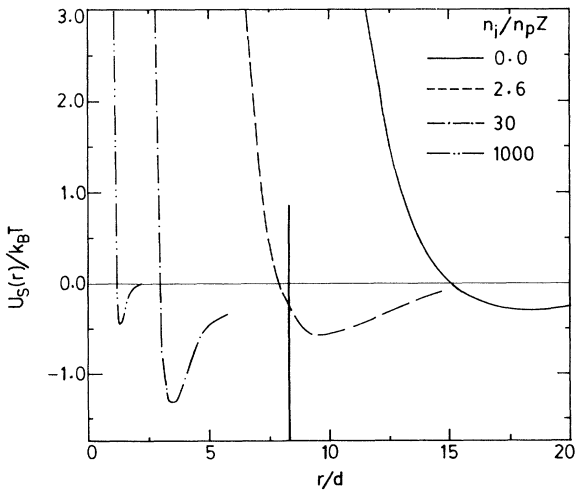

FIG. 1. The pair potential $U_S(r)/k_BT$ for different impurity-ion concentrations. Curves ——, – – – –, —·—·— and —··—··— correspond to $n_i/n_pZ = 0$, 2.6, 30, and 1000, respectively. The vertical line corresponds to the average interparticle separation a_s.

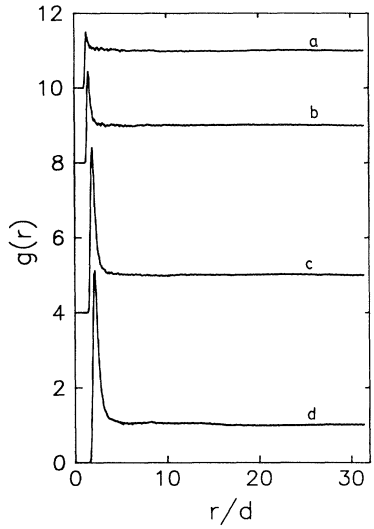

FIG. 2. $g(r)$ vs r for suspensions at high impurity-ion concentrations. Curves a, b, c, and d correspond to $n_i/n_pZ = 1000$, 400, 150, 100, respectively. Curves a, b, c are shifted vertically for the sake of clarity by the amounts 10, 8, and 4, respectively.

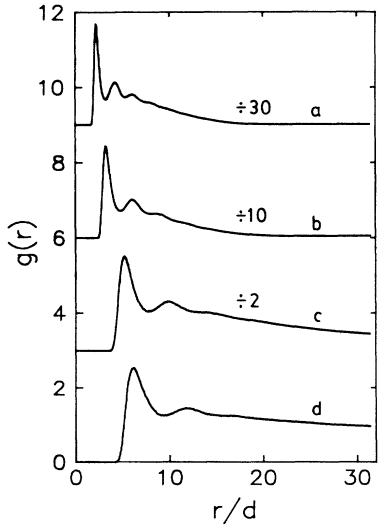

FIG. 3. $g(r)$ vs r for suspensions at intermediate impurity-ion concentrations. Curves a, b, c, and d correspond to $n_i/n_pZ = 78$, 30, 10, and 7, respectively. Curves a, b, and c, are compressed by factors 30, 10, and 2, respectively, and are shifted vertically for the sake of clarity. The vertical shift for curves a, b, and c correspond to 9, 6, and 3, respectively.

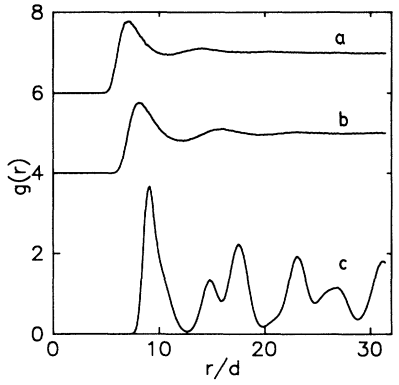

FIG. 4. $g(r)$ vs r for suspensions at low impurity-ion concentrations. Curves a, b, and c correspond to $n_i/n_pZ=5$, 3, and 0, respectively. Curves a and b are shifted vertically for the sake of clarity by the amounts, 6 and 4, respectively.

$n_i \leq 5n_pZ$ exhibit typical liquidlike behavior except that at $n_i=0$, which show a bcc crystalline order.

The appearance of peaks in pair-correlation functions at distances much shorter than a_s suggests the possibility of either clustering or formation of a condensed phase where $R_p \simeq R_m$. Clusters can remain homogeneously distributed all over the volume of the MC cell, whereas condensation would result in formation of large compact droplets of the dense phase, leaving the remaining volume practically empty. In order to find out the extent of clustering and/or condensation, clusters are identified using the procedure described in the previous section. Figures 5 and 6 show the cluster-size distribution for various values of n_i. Note that for $n_i=1000n_pZ$ only a few pairs are seen, and as n_i is reduced larger clusters are

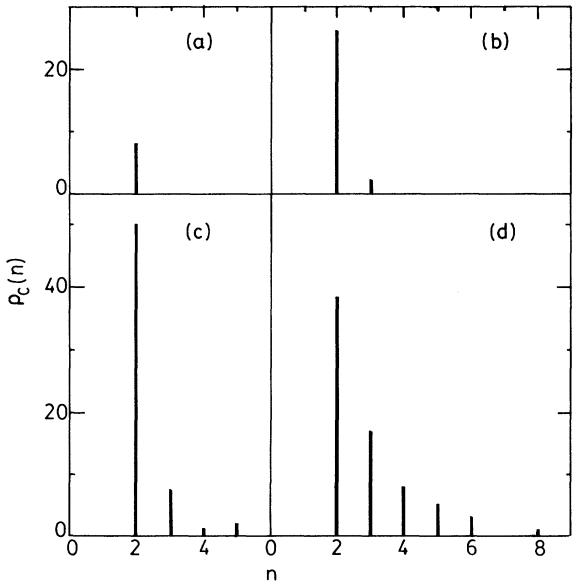

FIG. 5. Cluster-size distribution for suspensions at large n_i. (a), (b), (c), and (d) correspond to $n_i/n_pZ=1000$, 400, 150, and 100, respectively.

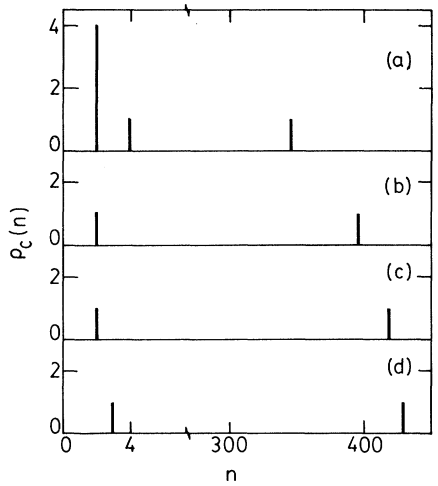

FIG. 6. Cluster-size distribution for suspensions at intermediate n_i. (a), (b), (c), and (d) correspond to $n_i/n_pZ=78$, 30, 10, and 7, respectively.

observed and the fraction F_c of particles participating in clustering also increases. Table II gives the values of various equilibrium parameters, like total interaction energy U_T, height $g_{\max}$ of the first peak in $g(r)$, F_c, and the osmotic pressure P^*. Note that F_c increases significantly as n_i decreases. The clustering behavior in suspensions with $7 \leq n_i/n_pZ \leq 78$ is also markedly different from that in systems with $n_i/n_pZ \geq 100$. Note from Fig. 6 that apart from a few small clusters, a large single cluster encompassing most of the particles is seen. This cluster, which exhibits pronounced short-range order, as seen in the corresponding $g(r)$'s, can be identified with a droplet of condensed phase. Figure 7 shows the projection of the coordinates of the particles in the MC cell onto the XY plane for suspensions with $n_i=1000$, 78, and $2.6n_pZ$. Note that the suspensions at high n_i and that at low n_i appear homogeneous, whereas that at $78n_pZ$ shows a droplet of condensed phase consistent with results shown in Fig. 6. Often a few particles are found to dissociate and reassociate from the dense-phase droplets during the MC evolution. Similar behavior of dissociation and reassociation has been noted in the case of smaller clusters as well. However, the total fraction F_c of particles constituting the clusters or the dense phase remains constant during further MC evolution. Figure 8 shows F_c as a function of MCS for suspensions with different n_i. The constancy of F_c for a system with $n_i=100n_pZ$ suggests a dynamical equilibrium between clusters and single particles. A similar inference can be made about the dense-phase droplet and single particles from the behavior of F_c for suspension at $78n_pZ$.

Based on the behavior of the pair-correlation function and the manner in which clustering occurs for suspensions with $n_i \geq 7n_pZ$, the systems can be grouped into two classes: (a) Suspension with $n_i \geq 100n_pZ$ exhibit small clusters without any structural correlation, and the cell volume is homogeneously occupied. One can see from Table II that for these systems P^* and $g_{\max}$ are low.

TABLE II. Monte Carlo simulation results after reaching equilibrium for suspensions at different n_i. The numbers in the parentheses represent error in the least significant digits. The abbreviations HG, HL, HC, and PS represent the homogeneous gas, homogeneous liquid, homogeneous crystalline, and phase-separated states, respectively.

n_i/n_pZ	U_T/Nk_BT	g_{max}	F_c (%)	P^*-1	State
0	57.18(9)	3.68(2)	100	33.70(4)	HC
1.5	−1.08(5)	2.23(2)	100	−6.39(4)	HL
2.0	−2.87(4)	2.03(2)	100	−7.42(5)	HL
2.6	−3.30(4)	1.81(2)	100	−7.39(4)	HL
3.0	−3.28(4)	1.75(2)	100	−7.10(6)	HL
5.0	−2.65(5)	1.76(2)	100	−5.58(5)	HL
7.0	−2.70(5)	2.54(2)	99.6	−5.58(6)	PS
10.0	−3.46(5)	5.00(3)	97.4	−7.08(4)	PS
30.0	−4.14(8)	24.38(12)	88.8	−9.86(7)	PS
78.0	−5.14(2)	80.71(35)	81.0	−11.52(9)	PS
100.0	−2.75(3)	5.14(3)	49.6	−0.60(4)	HG
150.0	−0.130(9)	4.40(4)	31.2	−0.35(5)	HG
400.0	−0.021(18)	2.43(4)	12.0	−0.065(6)	HG
1000.0	−0.0033(20)	1.48(4)	3.1	−0.014(4)	HG

Based on these features, the suspension can be characterized to be in a homogeneous vapor (gas) phase. (b) Suspensions with impurity-ion concentration in the range $78 \geq n_i/n_pZ \geq 7$ exhibit dense-phase droplets which have short-range structural correlations extending up to several neighbors and occupy only small regions of the simulation cell. The osmotic pressure and g_{max} are high for these suspensions. The gradual decay of $g(r)$ to one as r increases also reflects the boundary effects arising due to a compact droplet. These properties suggest that these suspensions can be considered to be a mixture of a condensed phase (liquidlike) in equilibrium with the vapor phase constituted by small clusters and free particles. Thus the colloidal suspension clearly exhibits a vapor-liquid condensation as the impurity-ion concentration is reduced. The results of present simulations are analogous to condensation of a gas in a container of fixed volume. It may be mentioned that this phenomenon occurs in atomic systems, e.g., in rare gases, when the temperature is lowered. The magnitude of the potential minimum relative to thermal energy k_BT determines the transition temperature [42]. In the case of colloids one can change the magnitude of interaction energy at any given distance at a fixed temperature simply by changing the impurity-ion concentration. Note from Table I that the depth of the potential minimum increases when n_i is reduced from 1000 to $78n_pZ$. Thus reduction of n_i is analogous to a reduction of equivalent temperature $T^*=W^{-1}$. Hence the occurrence of a vapor-liquid con-

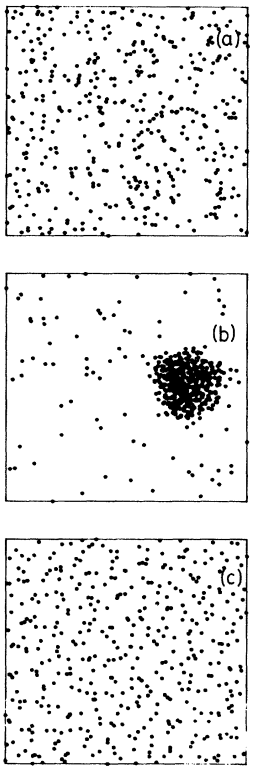

FIG. 7. Projection of coordinates of the particles in the MC cell onto the XY plane for suspension with (a) $n_i=1000$, (b) 78, and (c) $2.6n_pZ$.

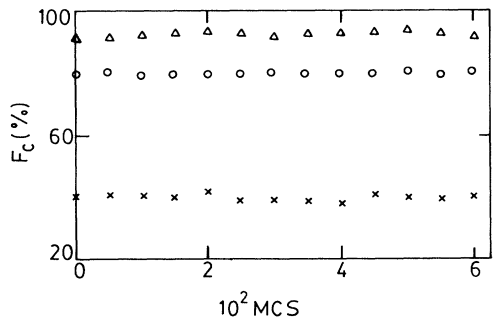

FIG. 8. Total fraction F_c of particles constituting the clusters or the dense phase as a function of MCS. The symbols Δ, ○, and × correspond to $n_i/n_pZ=30$, 78, and 100, respectively.

densation as a consequence of reduction of n_i is understandable.

Having identified the phases for suspensions with different n_i values, it is meaningful to identify the value of n_i at which the transition takes place. Figures 9 and 10 show the behavior of osmotic pressure and g_{max}, respectively, as a function of n_i. Note the sudden increase of both these parameters around $90n_pZ$ as n_i is reduced. This change is associated with the vapor-liquid condensation. The large values of these parameters arise due to scaling with respect to particle concentration n_p corresponding to the homogeneous dispersion instead of the particle concentration in the condensed phase n_d, which is several times higher than n_p. The dependence of P^* and g_{max} exhibit another discontinuous change at $n_i = 7n_pZ$. These quantities now exhibit increase as n_i is reduced. One can also see from Fig. 4 that the suspensions exhibit either liquidlike or crystalline structural ordering. Further, the suspensions again become homogeneous, as seen in Fig. 7. Hence the simulations predict a "subtle" transition from a phase-separated state to once again a homogeneous state. This can happen if the droplet of the condensed phase, which exhibits strong structural correlations, now expands to occupy the full volume of the simulation cell. This can be understood if one examines the behavior of R_m, which increases monotonically as n_i is reduced. Hence in the phase-separated state the volume occupied by the dense-phase droplets increases as n_i is decreased. Eventually, the droplet occupies the full volume of the MC cell as is evident from Fig. 1, which shows that $R_m > a_s$ at low impurity-ion concentrations. The behaviors of g_{max} and P^* suggest that the transition to this reentrant homogeneous state occurs at $7n_pZ$. MC simulations with $N=250$ at selected values of n_i also show the occurrence of the same phenomena, thereby establishing that the system size of $N=432$ is more than adequate for the present work. Thus the MC simulations carried out using the potential $U_S(r)$ predict a vapor-liquid condensation and a reentrant transition. It

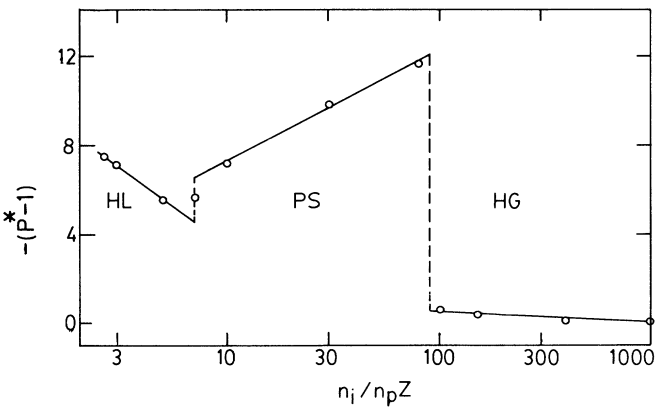

FIG. 9. $-(P^*-1)$ vs impurity-ion concentration n_i. HG, PS, and HL represent the homogeneous gaseous state, the phase-separated state, and the homogeneous liquid state, respectively. Lines drawn through the simulation points are guides to the eye.

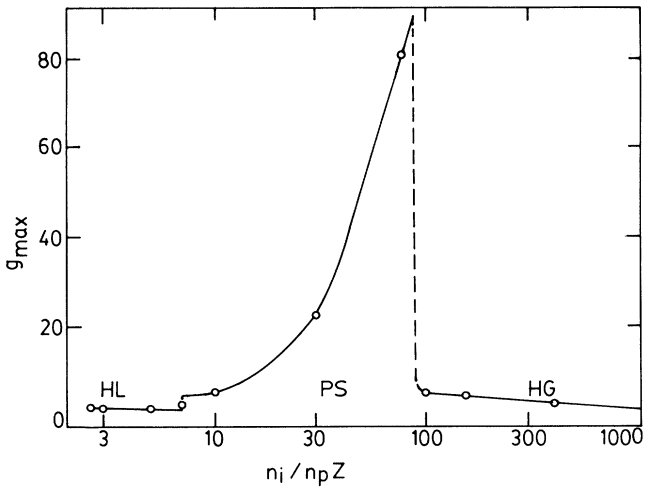

FIG. 10. Height g_{max} of the first peak of $g(r)$ as a function of n_i. Abbreviations HG, PS, and HL are the same as those in Fig. 9. Lines drawn through the simulation points are guides to the eye.

is important to point out that the reentrant transition at low n_i is unique to colloidal systems as it arises purely due to the specific dependence of the potential minimum on n_i. Atomic systems which have a fixed R_m do not exhibit this transition. As mentioned earlier, it is found that the suspension at $n_i=0$ is crystalline. Note from Table II that, in contrast to other suspensions, U_T and P^*-1 are positive in this case. This is because $R_m > a_s$ and the particles essentially see the repulsive edge of the potential. P^* being negative at finite n_i is due to the attractive part dominating over the repulsive part [42].

It is important to point out that the results of the present simulations are in complete agreement with those observed experimentally [9], i.e., (a) phase separation of weakly interacting homogeneous suspension upon deionization, (b) an increase of the volume occupied by the dense phase as n_i is reduced, and (c) an eventual reentrant transition to the strongly interacting homogeneous state upon further deionization. It may be mentioned that the experimental observations were earlier qualitatively understood on the basis of a free-energy calculation using the potential $U_S(r)$ [9]. It may be mentioned that for a particle concentration of 1.33×10^{12} cm^{-3} (volume fraction $\varphi \simeq 10^{-3}$), free-energy calculations [9] predicted phase transitions at 300 and $3n_pZ$, whereas according to the present simulations these occur at 90 and $7n_pZ$. This difference can be attributed to assumptions involved in the calculation of total interaction energy and entropy in the previous work [9]. We believe that the present MC results give a more realistic description of the system and better physical insight into the phenomena.

It may be pointed out that the recent observation of isolated bound pairs in dilute aqueous polystyrene suspensions [30] is also consistent with the prediction of MC results, as evident from the cluster-size distribution (see Figs. 5 and 6). One can see that the suspensions in the homogeneous vapor phase as well as in the phase-separated state have bound pairs. Only the fraction of

particles forming the bound pairs changes as a function of n_i. It is worth mentioning that subsequent to the report of reentrant phase transition [9] we have carried out further experiments on aqueous polysterene colloids with particle concentrations over a wide range using an angle-resolved polarized-light-scattering technique [45]. These experiments clearly demonstrate a vapor phase coexisting in equilibrium with a liquid-like phase and are in excellent agreement with the MC simulation results.

IV. CONCLUSIONS

The present simulations show a homogeneous liquid, a phase-separated state, and a homogeneous gas phase as the impurity concentration is varied, suggesting a reentrant phase transition, in confirmity with the observed experimental results in these systems. The reentrant phase transition arises as a consequence of the dependence of the position of the potential minimum on inverse Debye screening length. Vapor-liquid coexistence is found to occur for a certain range of impurity-ion concentrations, which is in complete agreement with recent experimental observations.

ACKNOWLEDGMENTS

B. V. R. Tata and A. K. Arora are indebted to Professor A. K. Sood for suggesting the problem, numerous stimulating discussions and helpful suggestions. They also gratefully acknowledge him for his keen interest during the entire course of this work. It is also a pleasure to thank Dr. G. Ananthakrishna and Dr. K. P. N. Murthy for helpful discussions and Dr. K. Krishnan for encouragement.

[1] For a recent review see A. K. Sood, in *Solid State Physics,* edited by H. Ehrenreich and D. Turnbull (Academic, New York, 1991), Vol. 45, p. 1.
[2] C. A. Castillo, R. Rajagopalan, and C. S. Hirtzel, Rev. Chem. Eng. **2**, 237 (1984).
[3] P. N. Pusey, Philos. Trans. R. Soc. London, Ser. A **293**, 429 (1979).
[4] B. V. R. Tata, R. Kesavamoorthy, and A. K. Sood, Mol. Phys. **61**, 943 (1987).
[5] R. Williams and R. S. Crandall, Phys. Lett. **48A**, 225 (1974).
[6] H. M. Lindsay and P. M. Chaikin, J. Chem. Phys. **76**, 3774 (1982).
[7] J. C. Brown, P. N. Pusey, J. W. Goodwin, and R. H. Ottewill, J. Phys. A **8**, 664 (1975).
[8] R. Kesavamoorthy, A. K. Sood, B. V. R. Tata, and A. K. Arora, J. Phys. C **21**, 4737 (1988).
[9] A. K. Arora, B. V. R. Tata, A. K. Sood, and R. Kesavamoorthy, Phys. Rev. Lett. **60**, 2438 (1988).
[10] E. J. W. Verwey and J. Th. G. Overbeek, *Theory of the Stability of Lyophobic Colloids* (Elsevier, Amsterdam, 1948).
[11] M. O. Robbins, K. Kremer, and G. S. Grest, J. Chem. Phys. **88**, 3286 (1990).
[12] R. O. Rosenberg and D. Thirumalai, Phys. Rev. A **36**, 5690 (1987).
[13] M. K. Udo and M. F. de Souza, Solid State Commun. **35**, 907 (1980).
[14] A. K. Arora, and R. Kesavamoorthy, Solid State Commun. **54**, 1047 (1985).
[15] J. G. Daly and R. Hasting, J. Phys. Chem. **85**, 294 (1981).
[16] P. N. Pusey, J. Phys. A **12**, 1805 (1979).
[17] F. Grüner and W. P. Lehmann, J. Phys. A **15**, 2847 (1982).
[18] N. Ise, T. Okubo, M. Sugimura, K. Ito, and H. J. Nolte, J. Chem. Phys. **78**, 536 (1983).
[19] N. Ise, H. Matsuoka, and K. Ito, Macromol. **22**, 1 (1989).
[20] K. Ito, K. Nakamura, and N. Ise, J. Chem. Phys. **85**, 6136 (1986).
[21] K. Ito, K. Nakamura, and N. Ise, J. Chem. Phys. **85**, 6143 (1986).
[22] N. Ise, K. Ito, T. Okubo, S. Dosho, and I. Sogami, J. Am. Chem. Soc. **107**, 8074 (1983).
[23] H. Yoshida, K. Ito, and N. Ise, J. Am. Chem. Soc. **112**, 597 (1990).
[24] K. Ito, H. Nakamura, H. Yoshida, and N. Ise, J. Am. Chem. Soc. **110**, 6955 (1988).
[25] H. Yoshida, K. Ito, and N. Ise, Phys. Rev. B **44**, 435 (1991).
[26] N. Ise, H. Matsuoka, and K. Ito, in *Ordering and Organization in Ionic Solutions,* edited by N. Ise and I. Sogami (World Scientific, Singapore, 1988), p. 397.
[27] R. Kesavamoorthy, M. Rajalakshmi, and C. Babu Rao, J. Phys. Condens. Matter **1**, 7149 (1989).
[28] N. Ise, H. Matsuoka, K. Ito, and H. Yoshida, Faraday Discuss. Chem. Soc. **90**, 153 (1990).
[29] N. Ise, K. Ito, and H. Yoshida, Polymer Preprints **33**, 769 (1992).
[30] S. Yoshino, in *Ordering and Organization in Ionic Solutions* (Ref. [26]), p. 449.
[31] M. Medina-Noyola, and D. A. McQuarrie, J. Chem. Phys. **73**, 6279 (1980).
[32] G. N. Patey, J. Chem. Phys. **72**, 5673 (1980); R. Kjellander and S. Marcelja, Chem. Phys. Lett. **112**, 49 (1984); J. Chem. Phys. **82**, 2122 (1985).
[33] B. Jönsson and H. Wennerström, in *Micellar Solutions and Microemulsions: Structure, Dynamics, and Statistical Thermodynamics,* edited by S. -H. Chen and R. Rajagopalan (Springer-Verlag, New York, 1990), p. 51.
[34] B. Svensson and B. Jönsson, Chem. Phys. Lett. **108**, 580 (1984).
[35] I. Sogami and N. Ise, J. Chem. Phys. **81**, 6320 (1984); I. Sogami, Phys. Lett. **96A**, 199 (1983).
[36] M. V. Smalley, Mol. Phys. **71**, 1251 (1990).
[37] J. Th. G. Overbeek, J. Chem. Phys. **87**, 4406 (1987).
[38] B. V. R. Tata, A. K. Sood, and R. Kesavamoorthy, Pramana J. Phys. **34**, 23 (1990).
[39] M. Matsumoto and Y. Kataoka, in *Ordering and Organization in Ionic Solutions* (Ref. [26]), p. 574.
[40] K. Ito, K. Sumaru, and N. Ise, Phys. Rev. B **46**, 3105 (1992).
[41] K. Binder, in *Monter Carlo Methods in Statistical Physics,* edited by K. Binder (Springer-Verlag, New York, 1979), p. 1.
[42] J. P. Hansen and I. R. McDonald, *Theory of Simple*

Liquids, 2nd ed. (Academic, London, 1986).
[43] C. S. Hirtzel and R. Rajagopalan, in *Micellar Solutions and Microemulsions: Structure, Dynamics and Statistical Thermodynamics* (Ref. [33]), p. 111.
[44] H. Müller-Krumbhaar, in *Monte Carlo Methods in Statistical Physics,* edited by K. Binder (Springer-Verlag, New York, 1979), p. 195.
[45] B. V. R. Tata, M. Rajalakshmi, and A. K. Arora, Phys. Rev. Lett. **69**, 3778 (1992).